DOI: https://doi.org/10.37434/tpwj2023.11.02

INFLUENCE OF GMAW AND PAW METHODS OF ADDITIVE ARC SURFACING AND SHIELDING GAS COMPOSITION ON SURFACE GEOMETRY AND METAL STRUCTURE OF PRODUCTS FROM LOW-CARBON 09G2S STEEL

V.V. Kvasnytskyi, I.M. Lahodzinskyi

National Technical University of Ukraine "Igor Sikorsky Kyiv Polytechnic Institute"
37 Prospect Beresteiskyi (former Peremohy), 03056, Kyiv, Ukraine

ABSTRACT

With the development of Wire Arc Additive Manufacturing (WAAM) technologies, there is a need in ensuring stable quality characteristics of spatial products, and it is desirable to obtain a final surface with minimal geometrical nonuniformity. Arc surfacing, in particular the process with short-circuiting (Cold Metal Transfer — CMT), and pulse-arc surfacing (Pulse process) allow improving the control of weld pool melt behaviour, and reducing material losses for spatter and burn-out, which ensures higher productivity of the process. At the same time, investigations of the regularities of the influence of arc melting methods, in particular CMT, Pulse and PAW technologies, and the composition of shielding gas atmosphere on the formed layer geometry, deposited metal structure and proneness to defect formation are urgent. Analysis of specimen geometry indicates that the shielding gas mixture composition has an essential influence on the deposited layer height, irrespective of the surfacing method (CMT/Pulse). Thus, for M11 mixture, the height of individual beads increases by 0.4–11.7 %, compared to the use of M21 mixture. Application of pulsed current leads to 10–11 % increase in the bead width, compared to CMT process. Metallographic examinations reveal that the metal product structure is typical for multilayer surfacing. A clear boundary between the individual deposited metal layers was not revealed.

KEYWORDS: WAAM, GMAW, Cold Metal Transfer, plasma, additive technologies, 09G2S, layer-by-layer surfacing, shielding gas mixture

INTRODUCTION

The rapid development of industry requires optimization of the existing technological processes of manufacturing not only individual products (prototypes, models), but also serial ones. However, from the point of view of serial manufacturing, there is a problem of the ratio of the cost of raw materials spent on the fabrication of a product and the cost of a final product. I.e., the amount of wastes remaining after the final processing of a product significantly affects the cost of each unit of a finished product. In other words, it is necessary to reduce the BTF — Buy to Fly ratio, which is used in the aerospace industry, which will provide a reduction in the amount of waste after final treatment [1].

Wire Arc Additive Manufacturing (WAAM) is a kind of additive manufacturing technology based on the use of arc heat sources and a compact filler material [2]. The processes of additive arc manufacturing using an electric arc (WAAM) are based on the principle of layer-by-layer bead surfacing. In contrast to the welding process, where the main role is played by the penetration depth and filling of the edge preparation with filler metal, in additive processes, on the contrary, researchers are trying to obtain the smallest penetration of the base (substrate) and mixing of the metal of the next layer with the previous one. They are also trying to achieve the highest possible height when building each individual bead.

The technology of Gas Metal Arc Welding (GMAW) surfacing with a consumable electrode in shielding gases has gained a significant development. This method involves continuous feeding and melting of a solid cross-section wire in a shielding gas. Thus, surfacing is carried out with the help of electric arc heating and continuous melting of the filler wire, which is deposited to the base surface. The weld pool and arc exist in the atmosphere of active or inert shielding gases. The process makes it possible to widely adjust the mechanical properties of manufactured products by using a diverse range of welding consumables for surfacing. The main advantages of using GMAW technologies in additive manufacturing are sufficiently high accuracy of bead formation during the central (axial) feeding of the electrode wire; a small number of controlled parameters of the surfacing mode, which contributes to the ease of the process control and its automation; simplicity, availability and relatively low cost of equipment.

However, the mentioned processes also have a number of disadvantages: relatively large heat input compared to highly concentrated heat sources (laser, electron beam); presence of significant metal spattering in the process of surfacing when using typical

gases or methods [3]. In order to reduce the heat input into the preliminary formed layers, the technology of Cold Metal Transfer (CMT) and pulsed arc (Pulse) processes is successfully used [4]. Regulation of the heat input allows a significant expansion of the range of materials suitable for GMAW technologies.

It is known that GMAW processes are characterized by quite significant nonuniformity of the surface produced by layer-by-layer formation [5]. The geometric accuracy and nonuniformity of the deposited layer surface are significantly influenced by surfacing modes, in particular, the value of current, arc voltage, filler wire feed rate and torch movement [6, 7]. It is also necessary to take into account the direction of the surfacing trajectory when generating subsequent layers [8]. A separate important influence parameter is the shielding gas mixture composition, since it is known that the presence of oxygen changes the value of the surface tension of the weld pool metal melt.

The main role of gas mixtures in GMAW processes consists in shielding the weld pool metal melt from interaction with environmental gases. Also, the shielding gas composition significantly affects the degree of arc gap ionization and, as a result, the arc burning stability. The authors of [9] confirmed the influence of the shielding gas composition on the process of metal transfer through the welding arc and on the geometric shape of deposited beads. The issue of the influence of shielding gas mixture components on the formation of shapes and surface nonuniformity during additive growing of products was considered in [10] regarding products of low-carbon steel of type 09G2S. The authors note that the thermal conductivity of each specific gas in the mixture also has a significant impact on the surface nonuniformity. Thus, gases with the lowest value of thermal conductivity, in particular Ar, contribute to lower heat input and, as a result, spread of the weld pool metal. When applying the CMT process, a decrease in the deviation from the straightness of the bead generatrix in the vertical direction is achieved, and the losses of filler material on spattering are reduced, which increases the material utilization ratio. The authors of [11] also confirmed that gases with higher thermal conductivity, in particular He, when added to gas mixtures of Ar–CO_2 composition, although lead to a decrease in the arc spot radius, which contributes to the formation of narrower beads, they also cause an increase in the penetration depth of the preliminary formed layers. As a result, a significant deviation of the geometric shape of the formed product walls is observed during successive surfacing of the subsequent layers. From the point of view of effective use of the material, this effect is negative, as the amount of metal waste grows during final machining. In addition to the influence on the geometric shape of the beads, different gas mixtures significantly affect the formation of the deposited metal structure. Thus, in [12] the authors considered the effect of the content of carbon dioxide in the mixture with argon on the deposited metal structure formation for high-strength steels (with strength of up to 950 MPa). The authors determined the ratio of the content of acicular and Widmanstätten ferrite and found that with an increase in the concentration of CO_2, in the composition of shielding gas, the amount of Widmanstätten ferrite grows. In [13–15], based on the results of their own research, the authors confirmed the influence of the composition of gas mixtures on the formation of the deposited metal structure. In particular, in [13] a comparison of geometric characteristics and quantity of individual structural components in the deposited metal is given. An important characteristic is the amount of nonuniformity of the specimen surface, which requires the introduction of the necessary tolerance for surface treatment to obtain a finished product. However, when studying the influence of gas mixtures composition on geometric characteristics of deposited layers during additive surfacing, as a rule, only GMAW surfacing or its variant — CMT process are considered. The literature provides limited information on the influence of the gas environment composition when using the Pulse process [16].

The aim of the work is to establish the regularities of the effect of GMAW-CMT/Pulse and PAW methods of arc surfacing and the shielding gas environment composition on geometric characteristics of the surfaces of products of low-carbon 09G2S steel, the structure of the deposited metal and the proneness to defect formation.

To achieve the aim, it was necessary to complete the following tasks:

- to analyze the information available in the literature regarding the peculiarities of the formation of the geometric shape and structure of the metal, proneness to the formation of defects in the walls of products manufactured using WAAM technologies of additive manufacturing with heating of a compact filler material with arc heat sources;
- to produce specimens of a layer-by-layer deposited metal using GMAW-CMT/Pulse and PAW methods of arc surfacing in the environment of active gas M11 and M21 mixtures and a solid cross-section wire from low-carbon 09G2S steel;
- to investigate geometric characteristics of the surfaces of produced specimens;
- to investigate the features of the metal structure of specimens, produced by GMAW-CMT/Pulse and PAW methods of arc surfacing, and the proneness to defect formation.

PROCEDURE OF EXPERIMENTS

In the studies of GMAW and PAW surfacing, a test bench for surfacing rectilinear beads was used (Fig-

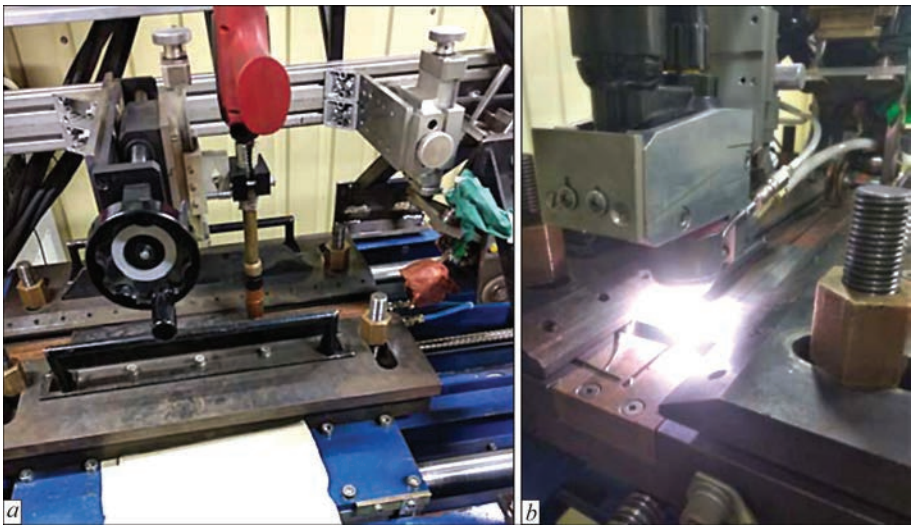

Figure 1. Test bench: *a* — suspended equipment for GMAW surfacing; *b* — plasma torch for PAW-CW surfacing

ure 1, *a*). As a power source, Fronius TransPulse Synergic 2700 unit in combination with PullMig CMT MHP 400i welding torch was used. For plasma surfacing, a specialized plasma torch was used, designed by NVTs Plazer LLC Company (Figure 1, *b*) in combination with Tetrix 421 power source and Fronius duty arc ignition module. The design of the torch provides a side feed of the filler wire and thus the process of PAW-CW (Cold Wire) surfacing is implemented. The filler wire was fed by a separate feed unit with a synchronous start. Surfacing of specimens by GMAW using Pulse and CMT methods was carried out by successive formation of individual layers in a reciprocating direction. For PAW method, the movement for each new layer formation is one-sided. The electrode wire diameter for all used grades of filler wires remained constant and amounted to d_e = 1.2 mm, the length of the formed walls was ~100 mm, the quantity of layers was 50.

Surfacing of layers by GMAW-CMT/Pulse methods was performed on 10 mm thick plates of E235-S (St3sp) steel. Layer-by-layer surfacing was performed with an electrode solid cross-section wire of type G3Sil (Sv-09G2S). To determine the influence of the gas shielding environment composition on geometric characteristics of the deposited layers and deposited metal structure formation during additive surfacing of low-carbon steels, the gas mixtures M21 (Ar 82 % + CO_2 18 %) and M11 (Ar 98 % + CO_2 2 %) were used as the most common in welding production. For each of the gas mixtures, surfacing of three specimens was performed using the CMT and Pulse methods.

Specimens were also produced by plasma-arc surfacing of a solid cross-section wire. The method of PAW-CW (Cold Wire) surfacing was used to manufacture specimens from low-carbon steel. The specimens were deposited on the substrates in the form of plates from E 235-S (St3sp-killed) steel of 10 mm thickness. As a filler material, the wire of type G3Sil (Sv-09G2S) was used. Taking into account the features of the plasma torch, namely the possibility of a separate supply of the plasma-forming and shielding gas, argon was used as the plasma-forming gas, and as a shielding gas, M11 mixture (Ar 98 % + CO_2 %) was used. The modes of layer-by-layer surfacing of specimens are given in Table 1. The input energy of surfacing specimens was determined by calculation (Table 1).

When choosing the temperature conditions for surfacing of individual layers, the strategy of interlayer cooling to 120 °C, proposed in [17], was chosen. Cooling of each individual layer was carried out in order to avoid excessive overheating of preliminary deposited layers.

To avoid overheating and distortion of the metal structure, after surfacing specimens for micro- and macrostructure examinations were cut out from the formed walls by mechanical means with the use of a

Table 1. Modes of layer-by-layer arc surfacing of specimens

Method	Filler material	Shielding gas	Input energy, J/mm	Current, A	Voltage, V	Nozzle diameter, mm	Wire feed rate $V_{w.f}$, m/min	Surfacing rate V_s, mm/min	Gas flow rate, l/min
GMAW-CMT	G3Si1 (Sv-09G2S)	M21	157	131	12	16	3.5	600	15
		M11	146	133	11				
GMAW-Pulse		M21	240	120	20				
		M11	262	131	20				
PAW-CW		Ar	262	202	13	4	3.5	600	0.6
		M11							15

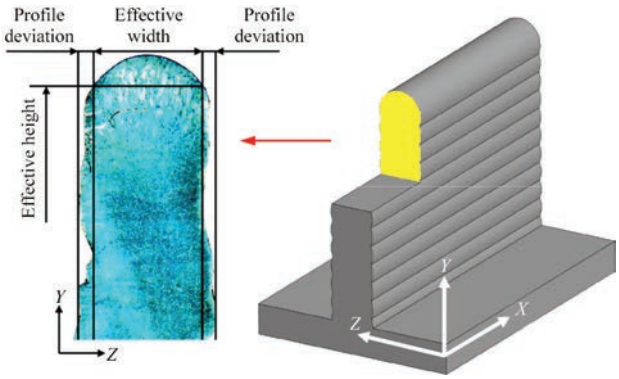

Figure 2. Determination of parameters of effective height, effective thickness and maximum profile deviation

lubricating and cooling liquid. Determination of the metal structure of the specimens was carried out by chemical etching in a 4 % alcoholic solution of nitric acid (HNO_3). The examinations were carried out in a Neophot-32 metallographic optical microscope. Metallographic examination of nonmetallic inclusions in the metal was carried out according to the scales of GOST 1778–70. The determination of grain size was carried out by comparison with the scales of GOST 5639–82. The hardness of phase components was measured by the Vickers method by means of LECO M-400 microhardness tester.

RESEARCH RESULTS AND THEIR DISCUSSION

The presented results of the analysis of changes in geometric characteristics of deposited specimens depending on the parameters of the surfacing modes, the applied method of GMAW surfacing (CMT or Pulse) in combination with different shielding environments are shown in Figures 3–6. These dependencies are quite important, because they are related to the amount of material spent on the finishing treatment of a generated billet of a product, since during additive surfacing, the shape of an almost finished part or a product with a tolerance for finishing is created. To evaluate geometric characteristics of products, the approach proposed in [10] using the effective height and effective wall width parameters was chosen (Figure 2). By analogy with tribotechnics, to evaluate geometric characteristics of the formed surface of products, the index of the maximum value of the wall profile deviation on both sides from the central axis is used (Figure 2). The smaller the deviation index, the closer the shape of a billet approximates to the shape of a finished product and the higher the efficiency of the material use. After all, during the final treatment, the tolerance for treatment and the material, which represents a scaly surface of a deposited product, go into waste.

A feature of the coarse of GMAW-CMT process (metal transfer with short circuits) is an almost complete exclusion of the phenomenon of metal spattering in the surfacing process. However, with a change in the gas mixture composition, the thermal conductivity of the gas environment and, as a result, the level of heat input into the welding pool are changed. Replacing the shielding gas from M21 mixture where 18 % CO_2 (Figure 3, *a*) to M11 with 2 % CO_2 (Figure 3, *b*) contributes to the reduction in the effective width of each individual deposited bead from 3.92 mm (for M21) to 3.68 mm (for M11). At the same time, the effective height of the wall increases from 68.1 mm in M21 mixture to 75.2 mm while using M11 mixture (Figure 6). From the point of view of the formed surface quality (Figure 3, *a*, *b*), the replacement of M21 gas mixture with M11 leads to a significant increase in the wall profile deviation indices (Figure 6). Considering the low thermal conductivity of argon by reducing its share in the mixture with carbon dioxide, which has a higher thermal conductivity, in combination with reduced heat input when applying the GMAW-CMT process, the weld pool life time is reduced. This leads to a decrease in the amount of remelted metal of the previous layers and a non-uniform spreading of the weld pool metal with a subsequent

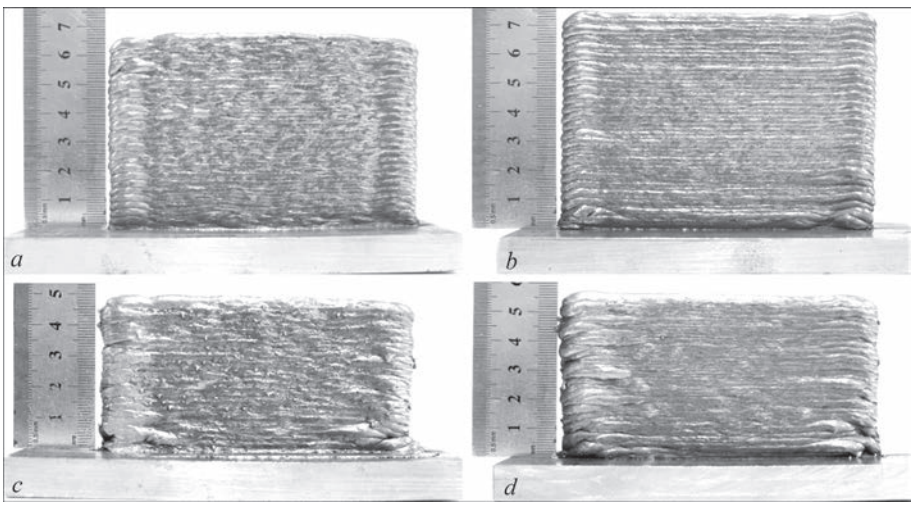

Figure 3. Specimens of low-carbon 09G2S (G3Sil) steel, produced by different surfacing methods using M21 and M11 gas mixtures: *a* — GMAW-CMT, M21 gas; *b* — GMAW-CMT, M11 gas; *c* — GMAW-CMT, M21 gas; *d* — GMAW-Pulse, M21 gas

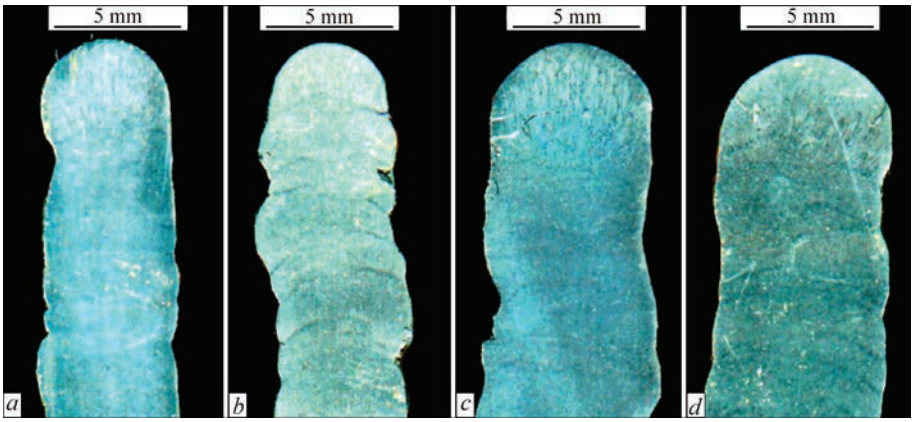

Figure 4. Macrostructure of specimens from low-carbon 09G2S (G3Sil) steel, produced by different surfacing methods using M21 and M11 gas mixtures: *a* — GMAW-CMT, M21 gas; *b* — GMAW-CMT, M11 gas; *c* — GMAW-CMT, M21gas; *d* — GMAW-Pulse, M21 gas

crystallization. This mechanism of influence of the thermal conductivity of the gas environment explains the relationship between the effective height, effective width and wall profile deviation, which is partially confirmed by the results of other studies [10].

The process of layer-by-layer formation of products with M21 gas mixture when applying the GMAW-Pulse process (Figure 3, *c*) is accompanied by active spattering of metal. Intense spattering is explained by the presence of a large amount (18 %) of carbon dioxide and a pulsed electric current supply [18]. Replacing the shielding gas environment by M11 (Figure 3, *d*) significantly reduces spraying during surfacing. As a consequence, in Figure 6, *a*, a clear dependence of the effective height of the wall on the composition of the used gas mixture can be observed. This dependence is similar to the results of surfacing obtained at the GMAW-CMT process.

Interesting is the dependence of changing the effective thickness of the wall on the composition of the gas environment. Thus, unlike the GMAW-CMT process (Figure 4, *a*, *b*), in the pulsed mode, the application of M11 mixture leads to an increase in the effective thickness of the manufactured wall by 10–11 % . The value of the effective width reaches 5.1 mm (Figure 4, *d*) when using M11 mixture and is decreased compared to the specimens, produced with the use of M21 mixture — 4.8 mm (Figure 4, *c*). As in the case of effective height, this is associated with a significant decrease in metal losses for spattering while reducing carbon dioxide content in the gas mixture.

Changing the content of carbon dioxide in the mixture significantly affected the value of the side wall surface deviation profile. For M1 and M21 mixtures, deviations of the wall profile amount to 0.68–0.78 and 0.57–0.62 mm, respectively (Figure 6).

For comparison with GMAW-Pulse/CMT processes, the wall was made by PAW-CW surfacing with unchanged welding speed parameters (V_w = 600 cm/min) and wire feed speed (V_{wf} = 3.5 m/min) (Figure 5).

Figure 6 presents the results of research on determination of the dependence of the effective wall thickness (Figure 6, *a*) and effective wall height (Figure 6, *b*) of the specimens. The analysis of produced results shows that, compared to GMAW processes, the wall produced by PAW-CW surfacing has the smallest side surface deviation profile.

Microstructural analysis of low-carbon steel specimens was carried out on the sections cut out from three separate zones: the last deposited layer, the transition zone between the last layer and previous layers, the zone of previous remelted layers.

Small nonmetallic inclusions of a rounded shape were found in almost all specimens (Figure 7, *a*, *b*). During the metallographic examination, it was established that these inclusions are oxides and silicates, which are fairly uniformly distributed over the entire cross-section of the specimens. The number and size of detected inclusions is less than the size No. 1 (based on the scale according to GOST 1778–70). In addition to single inclusions, single chains (Figure 7, *b*, *d*) and compact clusters of oxide and silicate inclusions are also observed (Figure 7, *b*, *d*). In the specimens produced by GMAW-CMT/Pulse surfacing processes in the shielding M11 gas mixture, the inclusions have an

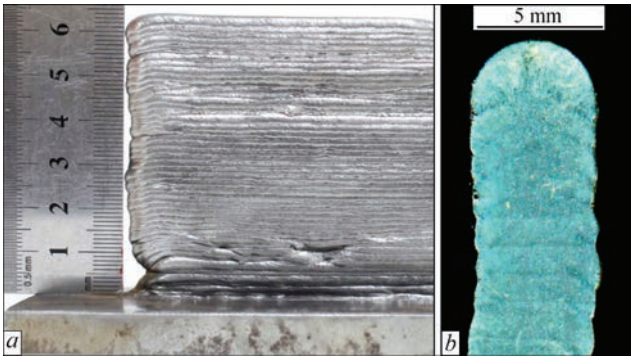

Figure 5. Specimen of 09G2S (G3Sil) steel deposited by the PAW-CMT method: *a* — general view of the side surface; *b* — transverse macrosection

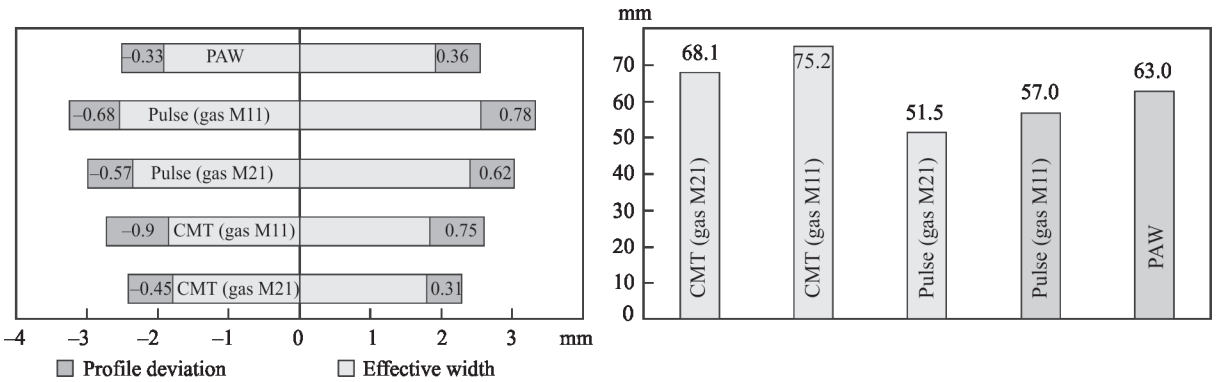

Figure 6. Dependence of the effective wall thickness (*a*) and their effective height (*b*) during additive surfacing of 09G2S steel (G3Sil) by GMAW-CMT/Pulse and PAW-CMT methods in shielding gas M21 and M11 mixtures

irregular shape, their composition differs from the composition of simple chemical compounds, in particular oxides and silicides (Figure 7, *c*). Their sizes exceed the sizes of oxides and silicates in these specimens.

The microstructure of the metal of the studied specimens of 09G2S (G3Sil) steel is characteristic of multilayer surfacings — the columnar structure of the cast metal, which indicates the orientation of crystallization from the liquid state, is observed only in the last deposited layer (Figure 8, *a*, *d*, *g*, *i*). The most finely dispersed structure (Figure 8, *a*–*c*) of the deposited metal is formed when using the GMAW-CMT method in combination with M21 gas mixture. The microstructure in the regions of the last surfacing layer is the precipitation of polygonal ferrite (sometimes with Widmanstätten orientation) and dispersed pearlite along the boundaries of the crystallites. The grain size number of the ferritic grain corresponds to Nos 9–10 according to GOST-5639–82. The share of Widmanstätten ferrite in the specimens deposited by the GMAW-Pulse method (Figure 8, *g*, *h*) is greater than in the specimens produced by GMAW-CMT surfacing with the same gas mixture. In the body of crystallites, several forms of ferrite are formed — polyhedral and two modifications of lamellar — with an ordered and a disordered second phase. Among themselves, the microstructure of the specimens differs in the size of the crystallites, the width of the polygonal ferrite precipitations along the boundaries of the crystallites and a number of other ferrite forms, as well as the microhardness of the deposited metal. The crystallite size ranges from: 80–130 μm for GMAW-Pulse method, 60–80 μm for GMAW-CMT with M21 gas and 80–160 μm for GMAW-CMT method in shielding M11 gas mixture.

The transition zone consists of the metal with a changed structure (overlapping area), which arose as a result of thermal effect when applying each subsequent layer. This zone mainly consists of fragmentary remnants of a directed columnar structure (Figure 8, *b*, *e*, *h*, *k*). The structure is refined, granular, ferritic-pearlitic with a significant content of ferrite. Thus, in the transition zone, the columnar structure of the deposited metal structure is violated, and a disoriented fine-grained structure is formed. In all specimens, a clearly defined boundary of the layers joint is not observed. Such a structure should have an increased fracture resistance.

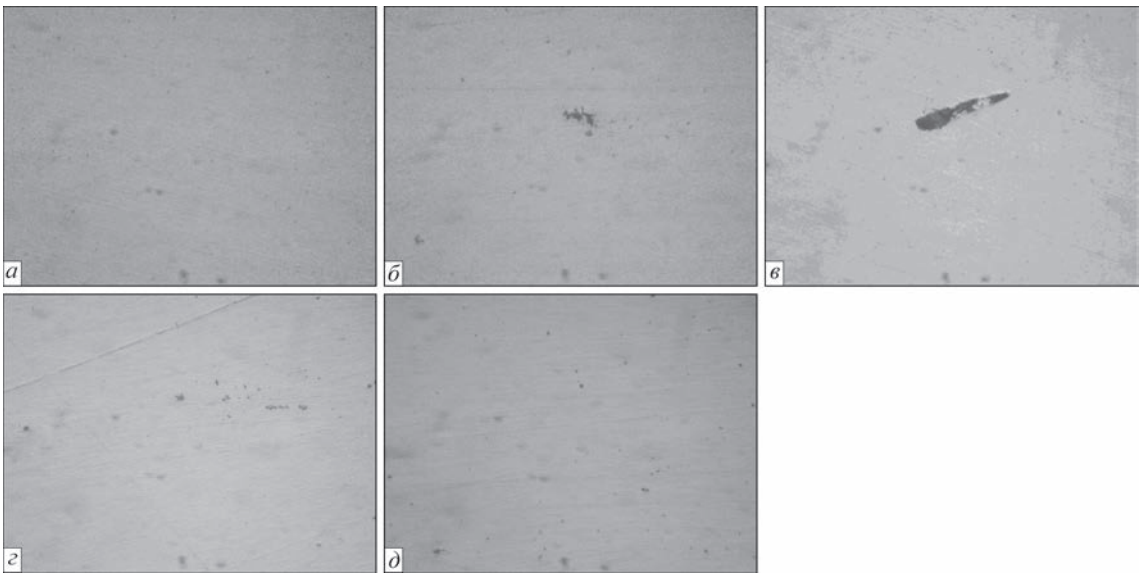

Figure 7. Microstructures (×100) of specimens from low-carbon 09G2S (G3Sil) steel, produced by different surfacing methods: *a* — GMAW-CMT, M21 gas; *b* — GMAW- CMT, M11 gas; *c* — GMAW-CMT, M21 gas; *d* — GMAW-Pulse, M21 gas; *e* — PAW-CW, M11 shielding gas, plasma-forming 100 % Ar

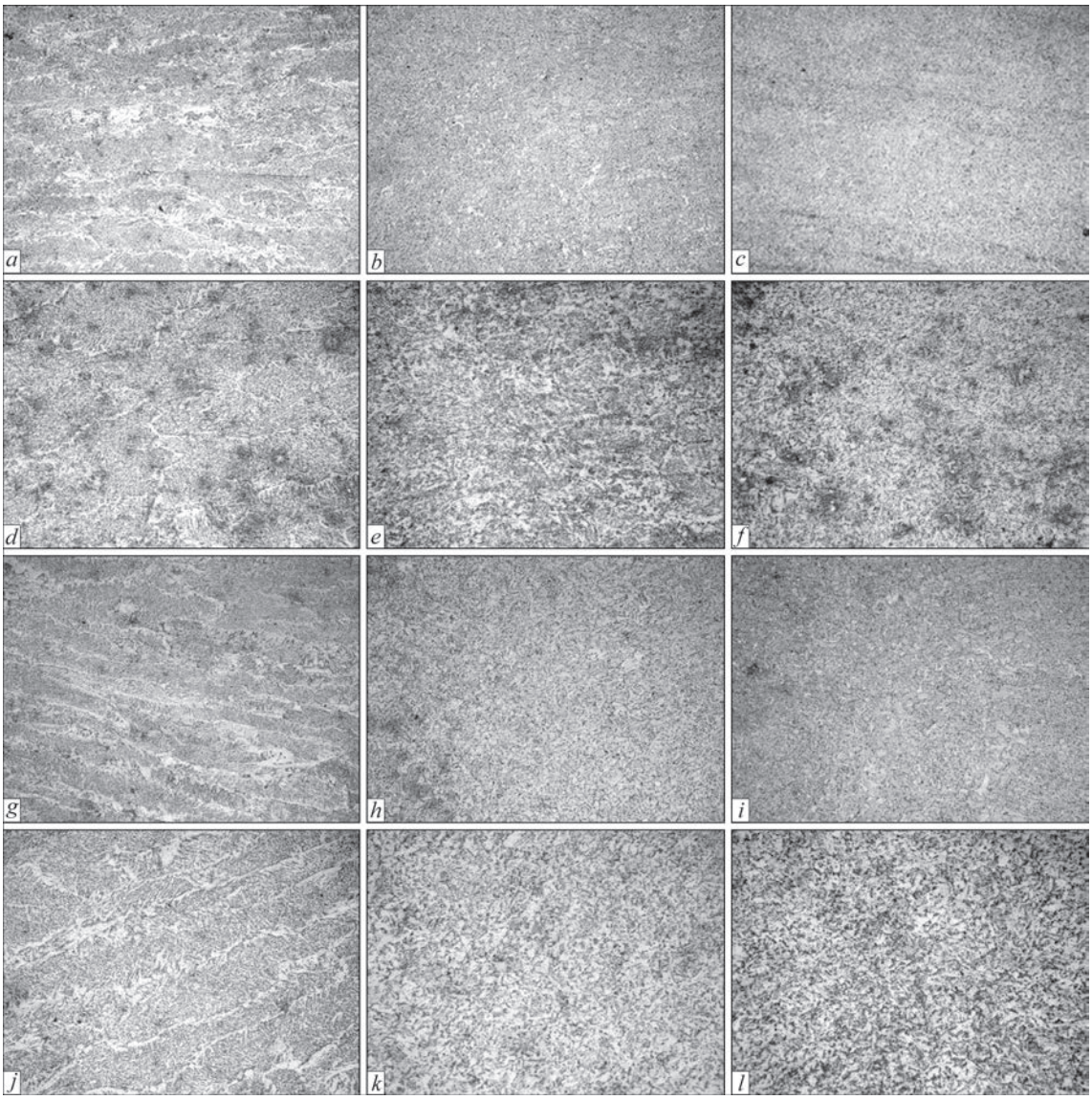

Figure 8. Microstructures (×800) of metal of specimens produced by layer-by-layer GMAW-CMT/Pulse surfacing in combination with different gas mixtures: *a* — GMAW-CMT, M21 gas; *b* — GMAW-CMT, M21 gas; *c* — GMAW-CMT, M21 gas; *d* — GMAW-CMT, M11 gas; *e* — GMAW-CMT, M11 gas; *f* — GMAW-CMT, M11 gas; *g* — GMAW-Pulse, M21 gas; *h* — GMAW-Pulse, M21 gas; *i* — GMAW-Pulse, M21 gas; *j* — GMAW-Pulse, M21 gas — the last deposited layer; *k* — GMAW-Pulse, M21 gas — transition zone; *l* — GMAW-Pulse, M21 gas — previous layers

In some places, the orientation of the structure, which is characteristic of cast metal, is preserved in the previous layers (Figure 8, *c*, *f*, *i*, *l*). The microstructure of the produced specimens differs in the size of the ferritic grain, in the transition zone and previous layers, the grain size Nos 7–8 according to GOST-5639–82 for the specimens produced by GMAW-Pulse, and No. 9 for GMAW-CMT surfacing.

The highest microhardness of the deposited metal on the HV1 scale is typical for specimens deposited by the GMAW-CMT method, when the shielding M11 gas mixture (1840–2082 MPa) is used. The microhardness of the specimens deposited with pulsed welding current supply varies within 1618–1922 MPa.

The microstructure of the metal of specimens deposited by the PAW-CW method is similar to the structure of specimens produced by GMAW-CMT/Pulse surfacing. The lowest microhardness of the metal among all tested specimens at the level of 1766–1885 MPa is observed in PAW-CW surfacing. The microstructure of the last layer consists of massive precipitations of polygonal ferrite, a significant part of which has a Widmanstätten orientation, and a dispersed pearlite distributed along the boundaries of the crystallites (Figure 9, *a*). The last layer consists of elongated dendrites. In the transition zone and the previous layer, an almost uniform area of overlapping layers is observed. The structure is ferritic-pearlitic, the amount of ferrite in the structure significantly exceeds the amount of pearlite (Figure 9, *b*). In the lower part of the deposited specimen, at a distance of about 1 mm from the substrate, a ferritic-pearlitic structure (Figure 9, *c*) with a grain size No. 9 is observed.

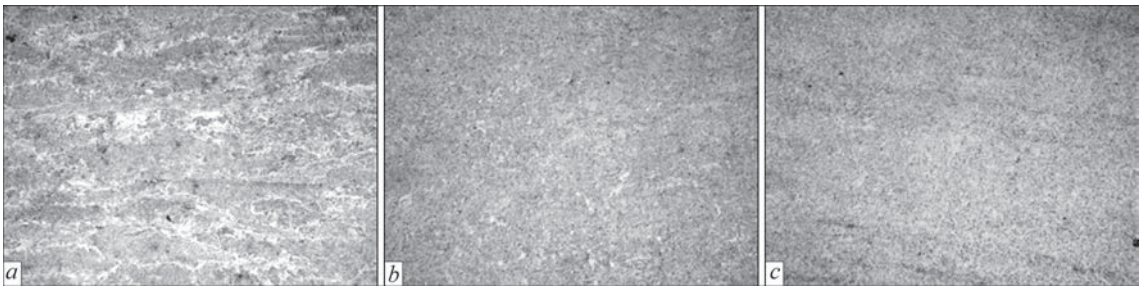

Figure 9. Microstructures (×800) of metal of specimen produced by layer-by-layer PAW-CW surfacing: *a* — last layer; *b* — transition zone; *c* — previous layers

Table 2. Average values of microhardness of deposited specimens, MPa

Method of surfacing and shielding gas mixture composition	Last layer		Transition zone	Previous layer
	Ferritic component	Body of crystals	Ferritic component	Ferritic component
GMAW-CMT (82 % Ar + 18 % CO_2)	1760	2032	1748	1602
GMAW-CMT (98 % Ar + 2 % CO_2)	2083	2238	1895	1840
GMAW-Pulse (82 % Ar + 18 % CO_2)	1923	2046	1740	1618
GMAW-Pulse (98 % Ar + 2 % CO_2)	1885	2093	1785	1766
PAW-CMT (shielding gas - 98 % Ar + 2 % CO_2) (plasma-forming gas - 100 % Ar)	1745	1812.5	1580	1687

The metal hardness of the deposited specimens is given in Table 2.

The analysis of the microhardness data of the phase component indicates the presence of the influence of the repeated passage of the heat source on the preliminary deposited layers. Thus, the microhardness of the previous layers decreases relative to the last layer as a result of repeated heating and subsequent tempering under the effect of the heat of the subsequent layers of deposited metal. The surface layers of the metal deposited by the GMAW-CMT method in M11 mixture with the wire G3Sil (09G2S) have a maximum hardness of about 2083 MPa.

CONCLUSIONS

1. The impact of CMT and Pulse methods of GMAW surfacing on geometric characteristics of deposited layers of G3Sil (09G2S) steel was determined. The largest height of the deposited specimens (~75 mm) during sequential surfacing of 50 layers and the minimum wall thickness of down to 4.6 mm is provided by GMAW-CMT surfacing. Replacing the shielding M11 gas mixture with M21 leads to a decrease in the wall height to 68 mm. The effective width of the metal walls deposited in M21 mixture is ~4 mm, and in M11 mixture it is ~3.6 mm. The replacement of M21 mixture with M11 is accompanied by a significant increase in profile deviation — from 0.31–0.45 to 0.75–0.9 mm. The formation of layers with the maximum height is associated with the lower heat input methods compared to other investigation methods, which leads to a decrease in the penetration depth of the metal of the preliminary deposited layer and a minimal spattering of the metal, especially in M11 mixture with a minimum content of CO_2.

2. In GMAW-Pulse surfacing of G3Sil (09G2S) steel, the height of the walls is minimal, and the effective width reaches the maximum values. Replacing the gas mixture from M11 to M21 leads to a decrease in the effective width of the walls with a simultaneous decrease in the deviation profile from 0.68–0.78 to 0.57–0.62 mm. The maximum values of the deviation profile are typical for GMAW surfacing when using M11 mixture. Plasma arc surfacing using cold wire (PAW-CW) provides intermediate values of the wall height of up to 63 mm and an effective width of ~4.4 mm. The profile deviation in PAW-CMT surfacing is minimal from the considered options and amounts to 0.33–0.36 mm.

3. In surfacing of low-carbon steel of G3Sil type (09G2S) GMAW-CMT/Pulse and PAW-CMT methods in all cases, a dense structure of the metal is formed, in which dispersed nonmetallic inclusions of oxides and silicates of a rounded shape were revealed, which are uniformly distributed over the entire cross-section of the specimens. The quantity and size of revealed inclusions is less than the size No. 1 (on the scale according to GOST 1778–70). In some regions, chains and compact clusters of inclusions are observed. The structure of the deposited metal is ferritic-pearlitic. The last deposited layer has a columnar structure that is typical of cast metal. In the transition zone, a disoriented fine-grained structure with fragmentary remnants of oriented columnar structures is observed, and in previously formed layers under the influence of subsequent

surfacing cycles, a disoriented fine-grained structure is formed. In all specimens, a clearly defined boundary of the layers joint is not observed.

4. The maximum values of microhardness are typical of the last deposited layers in all investigated methods and in GMAW-CMT surfacing in M11 gas mixture, they reach 2083–2238 MPa. The value of microhardness of the metal decreases when moving to the previously deposited layers, which is associated with the repeated action of the thermal cycle during multipass surfacing. In plasma surfacing, microhardness is minimal. For the last layer, it amounts to 1745–1813 MPa, and in the previously formed layers, the microhardness values of the metal decrease to 1580–1687 MPa.

REFERENCES

1. Ding, D., Pan, Z., Cuiuri, D. et al. (2016) Adaptive path planning for wire-feed additive manufacturing using medial axis transformation. *J. of Cleaner Production*, **133**, 942–952. DOI: https://doi.org/10.1016/j.jclepro.2016.06.036
2. Rodrigues, T.A., Duarte, V., Miranda, R.M. et al. (2019) Current status and perspectives on wire and arc additive manufacturing (WAAM). *Materials*, 12(**7**), 1121. DOI: https://doi.org/10.3390/ma12071121
3. Pan, Z., Ding, D., Wu, B. et al. (2018) Arc welding processes for additive manufacturing: A review. *Transact. on Intelligent Welding Manufacturing*, **1**, 3–24. DOI: https://doi.org/10.1007/978-981-10-5355-9_1
4. DebRoy, T., Wei, H.L, Zuback, J.S. et al. (2018) Additive manufacturing of metallic components — Process, structure and properties. *Progress in Materials Science*, **92**, 112–224. DOI: https://doi.org/10.1016/j.pmatsci.2017.10.001
5. Kvasnytskyi, V., Korzhyk, V., Lahodzinkyi, I. et al. (2020) Creation of volumetric products using additive arc cladding with compact and powder filler materials. In: *Proc. of 10th Inter. Conf. on Nanomaterials: Applications & Properties*, 02SAMA16-1–02SAMA16-5. DOI: https://doi.org/10.1109/NAP51477.2020.9309696
6. Xiong, J., Li, Y., Li, R., Yin, Z. (2018) Influences of process parameters on surface roughness of multi-layer single-pass thin-walled parts in GMAW-based additive manufacturing. *J. of Materials Processing Technology*, **252**, 128–136. DOI: https://doi.org/10.1016/j.jmatprotec.2017.09.020
7. Graf, M., Hälsig, A., Höfer, K. et al. (2018) Thermo-mechanical modelling of wire-arc additive manufacturing (WAAM) of semi-finished products. *Metals*, 8(**12**), 1009. DOI: https://doi.org/10.3390/met8121009
8. Ogino, Y., Asai, S., Hirata, Y. (2018) Numerical simulation of WAAM process by a GMAW weld pool model. *Weld World*, **62**, 393–401. DOI: https://doi.org/10.1007/s40194-018-0556-z
9. Rao, Z.H., Liao, S.M., Tsai, H.L. (2010) Effects of shielding gas compositions on arc plasma and metal transfer in gas metal arc welding. *J. of Applied Physics*, 107(**4**), 044902. DOI: https://doi.org/10.1063/1.3291121
10. Gurcik, T., Kovanda, K., Rohan, P. (2019) Influence of shielding gas on geometrical quality of WAAM technology. In: *Proc. of 28th Inter. Conf. on Metallurgy and Materials (METAL 2019)*, 715–721. DOI: https://doi.org/10.37904/metal.2019.871
11. Bishal, S., Pudasaini, N., Roy, S. et al. (2022) Altering the supply of shielding gases to fabricate distinct geometry in GMA additive manufacturing. *Applied Sciences*, 12(**7**), 3679. DOI: https://doi.org/10.3390/app12073679
12. Mvola, B., Kah, P. (2016) Effects of shielding gas control: Welded joint properties in GMAW process optimization. The International *J. of Advanced Manufacturing Technology*, 88(**9–12**), 2369–2387. DOI: https://doi.org/10.1007/s00170-016-8936-2
13. Gouda, M., Takahashi, M., Ikeuchi, K. (2005) Microstructures of gas metal arc weld metal of 950 MPa class steel. *Science and Technology of Welding and Joining*, 10(**3**), 369–377. DOI: https://doi.org/10.1179/174329305X40714
14. Menzel, M. (2003) The influence of individual components of an industrial gas mixture on the welding process and the properties of welded joints. *Welding Inter.*, 17(**4**), 262–264. DOI: https://doi.org/10.1533/wint.2003.3111
15. Ebrahimnia, M., Goodarzi, M., Nouri, M., Sheikhi, M. (2009) Study of the effect of shielding gas composition on the mechanical weld properties of steel ST 37-2 in gas metal arc welding. *Materials & Design*, 30(**9**), 3891–3895. DOI: https://doi.org/10.1016/j.matdes.2009.03.031
16. Zhao, Y., Shi, X., Yan, K. et al. (2018) Effect of shielding gas on the metal transfer and weld morphology in pulsed current MAG welding of carbon steel. *J. of Materials Processing Technology*, **262**, 382–391. DOI: https://doi.org/10.1016/j.jmatprotec.2018.07.003
17. Spencer, J.D., Dickens, P.M., Wykes, C.M. (1998) Rapid prototyping of metal parts by three-dimensional welding. Proceedings of the Institution of Mechanical Engineers, Pt B. *J. of Engineering Manufacture*, 212(**3**), 175–182. DOI: https://doi.org/10.1243/0954405981515590
18. Tokihiko, K., Rinsei, I., Koichi, Y., Yoshinori, H. (2009) Development of low spatter CO_2 arc welding process with high frequency pulse current. *Science and Technology of Welding and Joining*, 14(**8**), 740–746. DOI: https://doi.org/10.1179/136217109X449238

ORCID

V.V. Kvasnytskyi: 0000-0002-7756-5179,
I.M. Lahodzinskyi: 0000-0002-7986-9440

CONFLICT OF INTEREST

The Authors declare no conflict of interest

CORRESPONDING AUTHOR

V.V. Kvasnytskyi
E.O. Paton Electric Welding Institute of the NASU
11 Kazymyr Malevych Str., 03150, Kyiv, Ukraine.
E-mail: kvas69@ukr.net

SUGGESTED CITATION

V.V. Kvasnytskyi, I.M. Lahodzinskyi (2023) Influence of GMAW and PAW methods of additive arc surfacing and shielding gas composition on surface geometry and metal structure of products from low-carbon 09G2S steel. *The Paton Welding J.*, **11**, 21–29.

JOURNAL HOME PAGE

https://patonpublishinghouse.com/eng/journals/tpwj

Received: 25.10.2023
Accepted: 07.12.2023